

Impact of gapped spin-orbit excitons on low energy pseudospin exchange interactions

Sreekar Voleti,^{1,*} F. David Wandler,^{1,*} and Arun Paramakanti¹

¹*Department of Physics, University of Toronto, 60 St. George Street, Toronto, ON, M5S 1A7 Canada*
(Dated: March 9, 2023)

The quest for exotic quantum magnetic ground states, including the Kitaev spin liquid and quantum spin-ices, has led to the discovery of several quantum materials where low energy pseudospin-1/2 doublets arise from the splitting of spin-orbit entangled multiplets with higher degeneracy. Such systems include d -orbital and f -orbital Mott insulators. When the gap between the low energy pseudospin-1/2 levels and the excited levels of the multiplet or ‘excitons’ is not large, the effective low-energy exchange interactions between the low energy pseudospin-1/2 moments can acquire significant corrections from coupling to the excitons. We extract these corrections using higher order perturbation theory as well as an exact Schrieffer-Wolff transformation. Such corrections can impact the exchange matrix for the low energy pseudospin-1/2 levels by renormalizing the strength and the sign of Heisenberg exchange or Ising anisotropies, and potentially even inducing bond-anisotropic couplings such as Kitaev- Γ exchange interactions. We discuss recent experiments on various cobaltate and osmate materials which hint at the ubiquity and importance of this physics.

Magnetic solids exhibit strong quantum spin fluctuations in the limit of small spin. Spin-1/2 systems are thus natural candidates to look for exotic phases of quantum matter including quantum spin liquids. The simplest realization of such spin-1/2 degrees of freedom corresponds to single electrons nailed down at atomic sites in a single-orbital Mott insulating crystal. The low energy ordering and dynamics of such single-orbital Mott insulators can be described using effective Heisenberg models in the limit of strong Hubbard repulsion, with higher order ring-exchange terms becoming important for moderate Hubbard repulsion. A prototypical example is La_2CuO_4 [1–5], the undoped parent of the cuprate superconductors.

More interesting realizations of low-spin quantum magnets occur in multi-orbital systems with spin-orbit coupling (SOC), where the role of ‘spin’ is played by an effective pseudospin-1/2 moment with entangled spin and orbital degrees of freedom. The most well-studied example of this kind are the $j_{\text{eff}} = 1/2$ Mott insulators in compounds such as the layered Ir^{4+} perovskite iridate Sr_2IrO_4 [6–11], the layered honeycomb and hyperhoneycomb polytypes of A_2IrO_3 (with $\text{A}=\text{Li}, \text{Na}$)[12–14], or the analogue Ru^{3+} honeycomb ruthenate $\alpha\text{-RuCl}_3$ [15, 16]. In these cases, SOC splits the six-fold degenerate local t_{2g} orbitals (including spin) into a lower $j_{\text{eff}} = 1/2$ doublet with a significant gap $\sim 0.2\text{-}0.6\text{ eV}$ to the higher energy $j_{\text{eff}} = 3/2$ quartet which has been termed a ‘spin-orbit exciton’.

Here, we will focus on a distinct class of interesting pseudospin-1/2 magnets which appear in a variety of d -orbital transition metal oxides, and f -orbital heavy fermion materials, where the pseudospin doublet arises from weak splitting of a higher moment multiplet with SOC. A simple illustrative example is the case of a spin-3/2 multiplet which splits into a pair of Kramers doublets with $S_z = \pm 1/2$ and $S_z = \pm 3/2$ due to SOC in a tetragonal crystal. In this case, the lower Kramers doublet

acts as a low-energy pseudospin-1/2 degree of freedom while the upper doublet may be viewed as a ‘gapped exciton’. However, the exciton gap is not large. In order to understand the low energy emergent quantum phases of these pseudospin-1/2 magnets, we have to first extract the effective Hamiltonian describing the interaction between these doublets. This is commonly done by appealing to microscopic calculations of the two-site exchange interaction between the pseudospin-1/2 moments (e.g., from tight-binding models based on density functional theory), or tuning parameters of symmetry-based model spin Hamiltonians to fit experimental data from low energy probes such as inelastic neutron scattering. The reduction of the Hamiltonian from the full Hilbert space to the low energy pseudospin-1/2 Hilbert space is important to enable numerical studies on larger system sizes.

A key message of our work is that in Mott insulators where the splitting Δ between the low energy pseudospin-1/2 doublet and the ‘gapped exciton’ is not very large, the correct way to extract the two-site pseudospin exchange starting from an electronic Hamiltonian is via a two-step procedure. The first step involves second-order perturbation theory in the electron hopping which couples the entire pair of nearest neighbor multiplets. In Mott-Hubbard insulators, this results in a matrix of exchange couplings with an exchange scale $J_{\text{ex}} \propto t^2/U$ where t is used as a shorthand for the orbital-dependent electron hopping matrix elements, and U is used as a shorthand for scales arising from Kanamori interactions. The second step is to integrate out the higher levels of the multiplet, which are split off by Δ , leading to an effective pseudospin-1/2 model. This induces important exchange corrections which are on the scale of J_{ex}^2/Δ which is thus fourth-order in the electron hopping. We will discuss several examples showing how the resulting low energy effective Hamiltonian can differ significantly from the naive result where we project to the low energy doublet from the outset.

Quantum magnets which possess a pair of weakly split Kramers doublets can be realized in several octa-

* These authors contributed equally to this work

hedrally coordinated Mott insulators with SOC, so it is not an uncommon scenario. Examples of such systems include d^7 cobaltates such as CoTiO_3 which exhibits low energy Dirac magnons and dispersive spin-orbit excitons [17–19], and candidate Kitaev materials such as $\text{BaCo}_2(\text{AsO}_4)_2$, $\text{BaCo}_2(\text{PO}_4)_2$, $\text{Na}_3\text{Co}_2\text{SbO}_6$ and $\text{Na}_2\text{Co}_2\text{TeO}_6$ [19–26] These systems with strong trigonal distortion realize an effective spin $S=3/2$ moment which is split into two Kramers doublets by SOC. Other examples include d^1 Mott insulators such as $\text{Ba}_2\text{MgReO}_6$ which displays a higher temperature quadrupolar and lower temperature dipolar magnetic ordering transitions, and magnetically ordered d^3 materials such as $\text{Sr}_2\text{FeOsO}_6$ [27, 28] In these systems, the pair of Kramers doublets may arise, respectively, from tetragonal splitting of a $j=3/2$ or $J=3/2$ moment.

A distinct type of weakly split multiplet is realized d^2 Mott insulators which host an angular momentum $J=2$ multiplet that splits into a ground non-Kramers E_g pseudospin-1/2 doublet and an excited T_{2g} triplet even in an octahedral crystal field. Recent work has revealed osmate double perovskites such as Ba_2MOsO_6 ($M = \text{Zn}, \text{Mg}, \text{Ca}$) as candidates for realizing such non-Kramers doublets[29–33] In this case, the low energy τ_x and τ_z pseudospin operators transform as a two-component electric quadrupole, while τ_y transforms as an Ising magnetic octupole. These compounds appear to show some evidence for ferro-octupolar ordering of the non-Kramers doublets, while the higher energy T_{2g} triplet acts as a ‘gapped exciton’. In this case, the small E_g - T_{2g} exciton gap arises due to a combination of Hund’s coupling and SOC-induced virtual transitions from single-particle t_{2g} to e_g levels.

We will discuss several models where the coupling between the lower and upper multiplet significantly impacts the naive low-energy Hamiltonian. Using a two-step perturbation theory, we show that this can renormalize and even potentially flip the sign of the exchange couplings, or can generate entirely new bond-anisotropic terms such as Kitaev or off-diagonal Γ interactions. We test our two-step perturbative results against an exact Schrieffer-Wolff transformation. We note that similar ideas have also been explored in recent work with applications to Sr_2IrO_4 , and may also be relevant to anisotropic and higher-order spin interactions in heavy fermion systems.

I. EXTENDED PERTURBATION THEORY

Let us consider a D -dimensional multiplet at each site split by energy Δ into low energy ‘pseudospin’ multiplet of degeneracy D_L and a high energy ‘exciton’ multiplet of degeneracy $D_H = D - D_L$. For the case of spin-3/2 split into two Kramers doublets, $D=4$ and $D_L=D_H=2$. For the d^2 ion split into a non-Kramers pseudospin and a triplet exciton, we have $D=5$ with $D_L=2$ and $D_H=3$. When a neighboring pair of sites are connected by a hopping Hamiltonian H_T , the standard procedure for com-

puting the two-site pseudospin exchange involves treating H_T within second order perturbation theory, integrating out the intermediate charge transfer excitations which are at much higher energy $\sim U$ (the Hubbard interaction). This leads to a $D_L^2 \times D_L^2$ Hamiltonian matrix which can be recast in terms of exchange interaction parameters between the pseudospins. However, when Δ is small, in a manner to be clarified below, the correct procedure is a two-step approach. The first step is to extract the full $D^2 \times D^2$ Hamiltonian \mathcal{V}_J which espouses all second order contributions in H_T to exchange couplings between the entire J -multiplets (i.e., both pseudospins and excitons). The second step is to integrate out the high energy excitons and obtain an effective low-energy pseudospin Hamiltonian. Accordingly, we split up the full two-site multiplet Hamiltonian, obtained at the end of the first step above, as $\mathcal{H} = H_0 + \mathcal{V}_J$, where H_0 represents the on-site splitting Δ between the pseudospin and exciton levels, and V_J is $\mathcal{O}(t^2/U)$. This site-localized Hamiltonian H_0 has three distinct energy levels: (i) $E_0^{(0)}$ corresponding to both sites being in the pseudospin branch, (ii) $E_1^{(0)} = E_0^{(0)} + \Delta$ corresponding to one of the sites being in the exciton branch, and (iii) $E_2^{(0)} = E_0^{(0)} + 2\Delta$ when both sites live in the exciton branch. The degeneracies of these levels are D_L^2 , $2D_L D_H$, and D_H^2 respectively. Typically, the effective Hamiltonian between the sites is just extracted at $\mathcal{O}(t^2/U)$ as the projection of \mathcal{V}_J onto the $E^{(0)}$ manifold i.e. $H_{\text{eff}}^{[1]} = P_0 \mathcal{V}_J P_0$, where P_0 is the projector onto the $E^{(0)}$ subspace. The exciton-induced correction is given by

$$H_{\text{eff}}^{[2]} = P_0 \mathcal{V}_J P_1 \left(\frac{1}{E_0^{(0)} - H_0} \right) P_1 \mathcal{V}_J P_0 \quad (1)$$

where $P_1 = 1 - P_0$; this expression in Eq. (1) is *fourth* order in the hopping Hamiltonian H_T between the sites, and is typically ignored. While this term is $\sim \mathcal{O}(t^4/U^2\Delta)$, it can nevertheless become comparable to the conventional exchange coupling, when $\Delta \sim \mathcal{O}(t^2/U)$.

A. Split $J = 3/2$ moment

Here, we apply the extended perturbation theory to an effective split $J = 3/2$ system (i.e. with $D_L = D_H = 2$). Before exploring the physics, we establish a useful basis for the two-site problem. Using σ^a to denote the usual Pauli matrices [34], we define the following convenient basis for the 4×4 Hermitian matrices (written in the basis $\{|1/2\rangle, |-1/2\rangle, |3/2\rangle, |-3/2\rangle\}$) that can act on each site:

$$\eta^a = \begin{pmatrix} \sigma^a & 0 \\ 0 & 0 \end{pmatrix}, \quad \tau^a = \begin{pmatrix} 0 & 0 \\ 0 & \sigma^a \end{pmatrix}, \quad (2)$$

$$\xi_r^a = \frac{1}{\sqrt{2}} \begin{pmatrix} 0 & \sigma^a \\ \sigma^a & 0 \end{pmatrix}, \quad \xi_i^a = \frac{1}{\sqrt{2}} \begin{pmatrix} 0 & -i\sigma^a \\ i\sigma^a & 0 \end{pmatrix}. \quad (3)$$

Here, $a \in \{0, 1, 2, 3\}$ for each type of operator. In this basis, the η^a operate within the $J_z^2 = 1/2$ subspace, the τ^a operate within the $J_z^2 = 3/2$ subspace, and the ξ_r^a and ξ_i^a swap states between these two subspaces. These 16 matrices are more convenient than the usual $J = 3/2$ multipole operator basis, because they naturally separate the two doublets. See Appendix C for the change of basis to multipole operators.

For the purposes of integrating out the excitons to leading order, we only need the following terms from the $J = 3/2$ interaction Hamiltonian:

$$\begin{aligned} \mathcal{V}_J = & J_{ab}^{(\eta m)} \eta^a \eta^b + \sum_{s=r,i} K_{ab}^{(s)} (\eta^a \xi_s^b + \xi_s^b \eta^a) \\ & + \sum_{s,t=r,i} M_{ab}^{(st)} \xi_s^a \xi_t^b \end{aligned} \quad (4)$$

These three terms correspond to processes that do not excite an exciton, excite exactly one exciton, and excite two excitons, respectively. Other terms would annihilate states with no excitons, so they cannot contribute to the physics of the lower doublet at second order in perturbation theory (i.e. they would vanish when taking the projection via P_0 to the lower energy sector in Equation 1).

We are looking for an interaction matrix between the pseudospin-1/2 moments, which we call J_{eff} . This should be understood as the Hamiltonian

$$H_{\text{eff}} = \tilde{\mathbf{s}}_1^T J_{\text{eff}} \tilde{\mathbf{s}}_2 \quad (5)$$

where $\tilde{\mathbf{s}}$ refers to the vector of spin operators in the two dimensional pseudospin space, and the numbered subscript indicates the site index. The second order perturbation calculation can be done according to Equation (1), yielding:

$$J_{\text{eff}} = J^{(\eta m)} + \delta J_K + \delta J_M \quad (6)$$

where

$$\begin{aligned} (\delta J_K)_{ab} = & -\frac{1}{2\Delta} \left(K_{cd}^{(r)} - iK_{cd}^{(i)} \right) \left(K_{ef}^{(r)} + iK_{ef}^{(i)} \right) \\ & \times (\lambda_{cea} \lambda_{dfb} + \lambda_{ceb} \lambda_{dfa}) \end{aligned} \quad (7)$$

and

$$\begin{aligned} (\delta J_M)_{ab} = & -\frac{1}{8\Delta} \left(M_{cd}^{(rr)} - M_{cd}^{(ii)} - iM_{cd}^{(ri)} - iM_{cd}^{(ir)} \right) \\ & \times \left(M_{ef}^{(rr)} - M_{ef}^{(ii)} + iM_{ef}^{(ri)} + iM_{ef}^{(ir)} \right) \\ & \times \lambda_{cea} \lambda_{dfb} \end{aligned} \quad (8)$$

Here we have defined the lambda symbol by $\sigma^a \sigma^b = \lambda^{abc} \sigma^c$. Explicitly,

$$\lambda_{abc} = \begin{cases} \delta_{bc} & a = 0 \\ \delta_{ac} & b = 0 \\ \delta_{ab} & c = 0 \\ i\varepsilon_{abc} & a, b, c \neq 0 \end{cases} . \quad (9)$$

It is clear from these equations that having $K \sim \sqrt{J^{(\eta m)}} \Delta$ or $M \sim \sqrt{J^{(\eta m)}} \Delta$ could lead to changes on the order of $J^{(\eta m)}$. In Section IV, we will demonstrate some toy examples where this occurs and completely changes the physics of the resulting spin theory. For now we test extended perturbation theory on physically realistic models.

B. First application: Spin-3/2 with tetragonal distortion

Let us consider a $\tilde{S} = 3/2$ multiplet, where this large ‘spin’ might experience weak SOC, or arise as a strongly spin-orbit coupled $j = 3/2$ or $J = 3/2$ moment. We assume this is split into two Kramers doublets via a tetragonal distortion encapsulated by the Hamiltonian

$$H_0 = \Delta [\tau_0(\mathbf{r}) + \tau_0(\mathbf{r}') + 2\tau_0(\mathbf{r})\tau_0(\mathbf{r}')]. \quad (10)$$

Here, $\tau^0 = (Q_{z^2} + 1)/2$ with $Q_{z^2} = \tilde{S}_z^2 - \tilde{S}(\tilde{S} + 1)/3$. Let \mathcal{V}_J contain Heisenberg spin exchange, as well as quadrupole, and octupole interactions given by

$$\begin{aligned} \mathcal{V}_J = & \mathbb{J}_H \tilde{\mathbf{S}}(\mathbf{r}) \cdot \tilde{\mathbf{S}}(\mathbf{r}') + \mathbb{J}_Q Q_{xy}(\mathbf{r}) Q_{xy}(\mathbf{r}') \\ & + \mathbb{J}_T T_{xyz}(\mathbf{r}) T_{xyz}(\mathbf{r}') \end{aligned} \quad (11)$$

where $Q_{xy} = (\tilde{S}_x \tilde{S}_y + \tilde{S}_y \tilde{S}_x)/\sqrt{3}$ is the quadrupole operator, and $T_{xyz} = 2\text{Sym}[\tilde{S}_x \tilde{S}_y \tilde{S}_z]/3\sqrt{3}$ is the Ising-like octupole operator with ‘Sym’ denoting symmetrization. Let us denote pseudospin-1/2 operators acting on the low energy doublet as $\tilde{s}_\alpha = \sigma_\alpha/2$ where σ are Pauli matrices. A simple projection of the spin-3/2 Hamiltonian into this pseudospin-1/2 doublet leads to

$$H_{\text{eff,ex}}^{[1]} = \mathbb{J}_H (\tilde{s}_x^1 \tilde{s}_x^2 + \tilde{s}_y^1 \tilde{s}_y^2) + \frac{\mathbb{J}_H}{4} \tilde{s}_z^1 \tilde{s}_z^2. \quad (12)$$

which is completely devoid of any terms which include the impact of higher multipole interactions. However, using the extended perturbation theory result in Eq. (1), we find

$$\begin{aligned} H_{\text{eff,ex}}^{[2]} = & \left(\mathbb{J}_H - \frac{3\mathbb{J}_H(\mathbb{J}_Q - \mathbb{J}_T)}{4\Delta} \right) (\tilde{s}_x^1 \tilde{s}_x^2 + \tilde{s}_y^1 \tilde{s}_y^2) \\ & + \left(\frac{\mathbb{J}_H}{4} - \frac{39\mathbb{J}_H^2}{16\Delta} - \frac{\mathbb{J}_Q \mathbb{J}_T}{\Delta} \right) \tilde{s}_z^1 \tilde{s}_z^2 \end{aligned} \quad (13)$$

From the above, we can see that while the form of the couplings is the same, the coupling strengths have the potential of being strongly renormalized by the presence of the exciton if the multipole couplings $\mathbb{J}_Q, \mathbb{J}_T \sim \Delta$ or $\mathbb{J}_Q \mathbb{J}_T / \mathbb{J}_H \sim \Delta$. The right combination of the multipole couplings can strongly suppress the zz interaction, giving rise to a pure XY model, or even flip the sign of the XXZ anisotropy.

II. APPLICATION TO MICROSCOPIC CALCULATIONS

Here we provide examples of how the above protocol may be used in a typical microscopic calculation, and see how it produces markedly different results compared to the standard treatment outlined at the beginning of the previous section. We consider two cases: a d^1 honeycomb system subject to trigonal distortion, and a d^2 fcc system that hosts higher order multipole moments in its ground state. These cases both feature larger moments that are split to give a (pseudo)spin-1/2 ground state, are numerically tractable via an exact Schrieffer-Wolff transformation (as outlined in Ref. [33]) in order to assess the accuracy of the EPT approach. The microscopic Hamiltonian for both of the cases is

$$H_{\text{loc}} = H_{\text{CEF}} + H_{\text{SOC}} + H_{\text{int}} \quad (14)$$

which includes t_{2g-e_g} crystal field splitting, SOC, and electronic interactions, written in the orbital basis ($\{yz, xz, xy\}, \{x^2-y^2, 3z^2-r^2\}$). The CEF term is given by:

$$H_{\text{CEF}} = \sum_{\alpha, \beta} \sum_s A_{\alpha\beta} c_{\alpha s}^\dagger c_{\beta s} \quad (15)$$

where A is the local crystal field matrix written in the orbital basis, and s is the spin. The SOC term is of the one-body form:

$$H_{\text{SOC}} = \frac{\lambda}{2} \sum_{\alpha, \beta} \sum_{s, s'} \langle \alpha | \mathbf{L} | \beta \rangle \cdot \langle s | \boldsymbol{\sigma} | s' \rangle c_{\alpha s}^\dagger c_{\beta s'} \quad (16)$$

where $\boldsymbol{\sigma}$ refers to the vector of Pauli matrices, and \mathbf{L} are orbital angular momentum matrices. The operators $c_{\alpha s}$, $c_{\alpha s}^\dagger$ and $n_{\alpha s}$ destroy, create, and count the electrons with spin s in orbital α . The Kanamori interaction is given by

$$H_{\text{int}} = U \sum_{\alpha} n_{\alpha\uparrow} n_{\alpha\downarrow} + \left(U' - \frac{J_H}{2} \right) \sum_{\alpha > \beta} n_{\alpha} n_{\beta} \quad (17)$$

$$- J_H \sum_{\alpha \neq \beta} \mathbf{S}_{\alpha} \cdot \mathbf{S}_{\beta} + J_H \sum_{\alpha \neq \beta} c_{\alpha\uparrow}^\dagger c_{\alpha\downarrow}^\dagger c_{\beta\downarrow} c_{\beta\uparrow}$$

where U and U' are the intra- and inter-orbital Hubbard interactions, J_H is the Hund's coupling, and $\mathbf{S}_{\alpha} = (1/2)c_{\alpha s}^\dagger \boldsymbol{\sigma}_{s, s'} c_{\alpha s'}$. The operator $n_{\alpha} \equiv n_{\alpha\uparrow} + n_{\alpha\downarrow}$ counts the total number of electrons in orbital α . The spherical symmetry of the Coulomb interaction sets $U' = U - 2J_H$ [35].

A. d^1 ions in a honeycomb lattice

A single-ion ground state of the Hamiltonian in Eq. 14 with a single electron restricted to the t_{2g} sector, is a four-fold degenerate $J = 3/2$ manifold. A typical situation that arises in 2D materials is when this ion is

in an octahedral cage, and the octahedra are used to form a honeycomb lattice. A natural distortion axis for such a lattice is that along the octahedral [111] direction, corresponding to the direction perpendicular to the honeycomb plane. Such a distorted octahedron has, in addition to the usual t_{2g-e_g} splitting, the following term in the crystal field matrix:

$$\frac{\delta}{3} (L_x + L_y + L_z)^2$$

where δ is the distortion parameter. Restricting ourselves to the t_{2g} sector, the A matrix is given by

$$\begin{pmatrix} 0 & \delta & \delta \\ \delta & 0 & \delta \\ \delta & \delta & 0 \end{pmatrix}. \quad (18)$$

The effect of this distortion term is to split the $J = 3/2$ moment into two Kramers doublets, with $|\pm 1/2\rangle$ as the ground state doublet, and $|\pm 3/2\rangle$ the 'exciton', higher in energy by Δ , as shown in Fig. 1(a). To obtain the pseudospin exchange, we consider a two site model of such octahedra, connected via a hopping Hamiltonian of the form

$$H_T^\gamma = \sum_{\alpha\beta s} (T_{\alpha\beta}^\gamma c_{2\beta s}^\dagger c_{1\alpha s} + T_{\beta\alpha}^{\gamma\dagger} c_{1\alpha s}^\dagger c_{2\beta s}) \quad (19)$$

where T^γ is the hopping matrix for the γ bond. We consider a matrix for the z bond in the honeycomb inspired by the 90 degree bonding geometry in Ref. [36]:

$$T^z = \begin{pmatrix} 0 & t_1 & 0 \\ t_1 & 0 & 0 \\ 0 & 0 & t_2 \end{pmatrix}. \quad (20)$$

Here, t_1 , is the $yz-zx$ hopping, and t_2 is the $xy-xy$ hopping. The matrices for the x and y bonds can be obtained via C_3 rotation about the octahedral [111] axis. For the illustrative case, we consider $t_1 = -100$ meV, and $t_2 = 50$ meV, along with the single ion parameters $(\lambda, U, J_H) = (0.1, 2.5, 0.3)$ eV. In the lab frame (see SI for details), the low energy pseudospin exchange matrix takes an XXZ form:

$$H_{\text{spin}} = \mathbb{J}_{XY} (\tilde{s}_x^1 \tilde{s}_x^2 + \tilde{s}_y^1 \tilde{s}_y^2) + \mathbb{J}_{ZZ} \tilde{s}_z^1 \tilde{s}_z^2. \quad (21)$$

Figure 1(b-c) shows the values of these exchange parameters when calculated using EPT, contrasted with the conventional method of directly projecting down to the lower manifold (SOPT). The two approaches are also compared with the exact two site Schrieffer-Wolff calculation. It can be seen that the EPT is much closer to the exact calculation, and the methods give significantly different coupling values. While the SOPT Hamiltonian remains XXZ for all gap values, it can be seen that for $\Delta \sim 17$ meV, the spin Hamiltonian is actually a pure XY model. It can also be seen that for a small enough gap value, we approach a point where $\mathbb{J}_{XY} \approx -\mathbb{J}_{ZZ}$. At this point, performing a single sublattice spin rotation

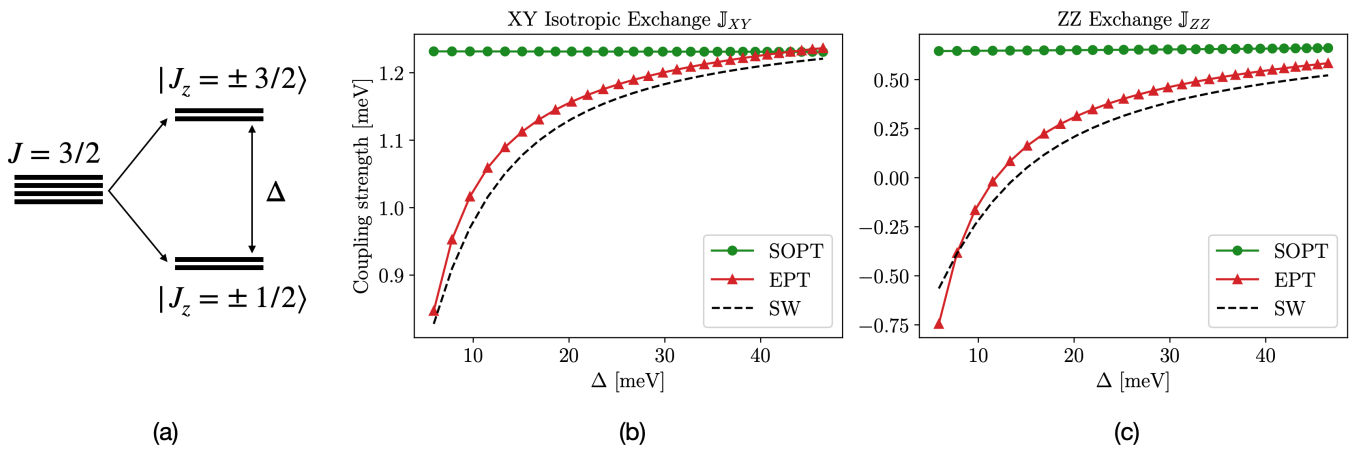


FIG. 1. (a) Level structure for a d^1 ion with spin-orbit coupling and trigonal distortion. The lower $|\pm 1/2\rangle$ states act as the effective spin-1/2 moment. (b),(c) Exchange couplings for the spin Hamiltonian in Eq. (21), computed using SOPT and EPT, and compared to the exact SW calculation.

such that ($\tilde{s}_x \rightarrow \tilde{s}_x$, $\tilde{s}_y \rightarrow -\tilde{s}_y$, $\tilde{s}_z \rightarrow -\tilde{s}_z$) would convert this into a pure Heisenberg antiferromagnet. Thus, the addition of the exciton mixing terms reveals a much richer class of spin Hamiltonians accessible via tuning the trigonal distortion.

B. d^2 ions in an fcc lattice

Another class of systems where this formalism is useful is those where the pseudospin degree of freedom is made up of non-Kramers states. These have recently been studied in the context of d^2 Double Perovskites, where a $J=2$ moment, when placed in a cubic environment, splits as $2(E_g) \oplus 3(T_{2g})$. The non-Kramers E_g ground state may be treated as a pseudospin 1/2 degree of freedom, with wavefunctions

$$|\psi_{g,\uparrow}\rangle = \frac{1}{\sqrt{2}}(|2\rangle + |-2\rangle); \quad |\psi_{g,\downarrow}\rangle = |0\rangle. \quad (22)$$

Within this non-Kramers doublet space, the Pauli matrices τ_x, τ_y, τ_z are proportional to multipole operators, and are given by $\tau_x \equiv (J_x^2 - J_y^2)/2\sqrt{3}$, $\tau_y \equiv \overline{J_x J_y J_z}/6\sqrt{3}$, and $\tau_z \equiv (3J_z^2 - J(J+1))/6$, with overline denoting symmetrization. Here, τ_x, τ_z are electric quadrupoles while τ_y is a magnetic octupole. [32]. The form of the pseudospin Hamiltonian has been shown to take the form

$$H_{\text{spin}} = \sum_{\langle i,j \rangle} [K_o \tau_{iy} \tau_{jy} + (K_1 \cos^2 \phi_{ij} + K_2 \sin^2 \phi_{ij}) \tau_{ix} \tau_{jx} + (K_1 - K_2) \sin \phi_{ij} \cos \phi_{ij} (\tau_{ix} \tau_{jz} + \tau_{iz} \tau_{jx}) + (K_1 \sin^2 \phi_{ij} + K_2 \cos^2 \phi_{ij}) \tau_{iz} \tau_{jz}] \quad (23)$$

where $\phi_{ij} = \{0, 2\pi/3, 4\pi/3\}$ correspond to nearest neighbors (i, j) in the $\{xy, yz, zx\}$ planes. K_o and $K_{1,2}$ respectively correspond to the octupolar exchange and

quadrupolar couplings. An exact two-site calculation using a Schrieffer-Wolff transformation to obtain the effective low energy Hamiltonian indicated that the nearby T_{2g} triplet is able to strongly influence the exchange parameters of the E_g doublets. This system thus provides with another testing ground for the EPT formalism. As shown in Figure 2(b-d), it can be seen that the dominant octupole-octupole exchange coupling shows a significant increase in magnitude, while also showing that the quadrupolar K_1 coupling is has the opposite sign and significantly higher magnitude compared to the SOPT case.

III. SOME INTERESTING TOY EXAMPLES

In addition to the above physically motivated examples, it is important to note that this extended perturbation theory can lead to wildly different physics from the naive second order predictions. In the case of a two doublet system, any conceivable change in spin models, δJ , can be realized with time-reversal invariant couplings between the doublets, with coupling coefficients in an intermediate scale between those of δJ and Δ . An explicit proof of this is given in Appendix B in the form of an algorithm that works backwards: taking any given δJ and working out a set of time-reversal invariant couplings that produce this δJ under perturbation theory. The system of equations that the algorithm solves is underdetermined meaning the results of this algorithm are not unique.

In the following subsections, we look at a few particularly striking cases with clean solutions. These demonstrate the power of inter-doublet couplings in changing the low energy physics.

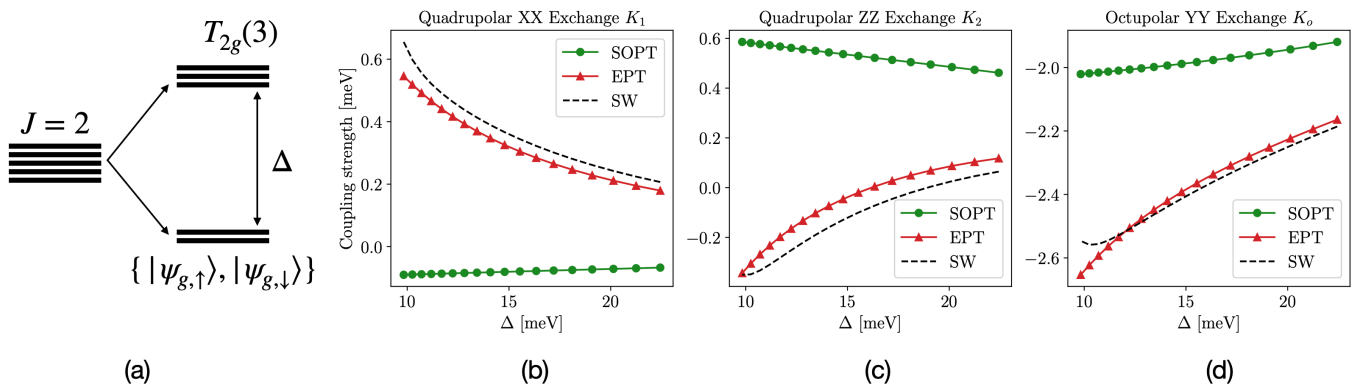


FIG. 2. (a) Level structure for a d^2 ion within a double perovskite crystal. (b),(c),(d) Exchange couplings for the pseudospin Hamiltonian in Eq. (23), computed using SOPT and EPT, and compared to the exact SW calculation.

A. Changing the Heisenberg coupling

To begin we consider the case where naive second order perturbation theory gives a Heisenberg (anti-)ferromagnet and the extended perturbation theory changes the strength or even the sign of the interaction. Hence, our starting spin model is

$$J = \begin{pmatrix} \mathcal{J} & 0 & 0 \\ 0 & \mathcal{J} & 0 \\ 0 & 0 & \mathcal{J} \end{pmatrix}, \quad (24)$$

with a correction of the form

$$\delta J = \begin{pmatrix} \kappa & 0 & 0 \\ 0 & \kappa & 0 \\ 0 & 0 & \kappa \end{pmatrix}. \quad (25)$$

Such a correction can be introduced using only $K^{(i)}$ couplings. For $\kappa > 0$, this can be achieved by introducing

$$K^{(i)} = \begin{pmatrix} 0 & 0 & 0 & 0 \\ 0 & \sqrt{\frac{\kappa\Delta}{2}} & 0 & 0 \\ 0 & 0 & \sqrt{\frac{\kappa\Delta}{2}} & 0 \\ 0 & 0 & 0 & \sqrt{\frac{\kappa\Delta}{2}} \end{pmatrix}, \quad (26)$$

and for $\kappa < 0$, this can be achieved by introducing

$$K^{(i)} = \begin{pmatrix} \sqrt{-2\kappa\Delta} & 0 & 0 & 0 \\ 0 & \sqrt{\frac{-\kappa\Delta}{2}} & 0 & 0 \\ 0 & 0 & \sqrt{\frac{-\kappa\Delta}{2}} & 0 \\ 0 & 0 & 0 & \sqrt{\frac{-\kappa\Delta}{2}} \end{pmatrix}. \quad (27)$$

Notice here that to completely reverse the sign of the interaction (and therefore change the physics from a ferromagnet to an antiferromagnet or vice versa), we need $\kappa = -2\mathcal{J}$, so the $K^{(r)}$ couplings introduced are on the order of $\sqrt{|\mathcal{J}|\Delta}$ which is the geometric mean of the spin interaction scale \mathcal{J} and the splitting scale Δ .

Figure 3 details the Δ dependence of this toy model for a particular choice of parameters. In particular, the parameters are chosen so that simple projection gives a ferromagnetic Heisenberg model, but extended perturbation theory gives an antiferromagnetic Heisenberg model with equal magnitude at $\Delta = 36\mathcal{J}$. The figure contrasts the standard projection with the extended perturbation theory. It also shows the results of integrating out the exciton with a Schrieffer-Wolff transformation. The full Hamiltonian used for this Schrieffer-Wolff transformation is the $J = 3/2$ toy model described above; therefore, unlike Figures 1 and 2, it gives no information regarding the agreement between EPT and an underlying microscopic model. Instead, the similarity between the EPT and SW results indicate that second order perturbation theory is sufficient to reliably extract to physical effects of the exciton from the $J = 3/2$ model.

B. Heisenberg to Kitaev

Consider a naive Heisenberg ferromagnet or antiferromagnet with second order spin model given by Equation 25. Such a material could have a significant Kitaev interaction in the presence of some $K^{(r)}$ couplings. For example, consider the couplings

$$K^{(i)} = \begin{pmatrix} 0 & 0 & 0 & 0 \\ 0 & \sqrt{\frac{\mathcal{K}\Delta}{2}} & 0 & 0 \\ 0 & 0 & \sqrt{\frac{\mathcal{K}\Delta}{2}} & 0 \\ 0 & 0 & 0 & -\mathcal{J}\sqrt{\frac{\Delta}{2\mathcal{K}}} \end{pmatrix} \quad (28)$$

with $\mathcal{K} > 0$. The extended perturbation theory including these couplings gives

$$\delta J = \begin{pmatrix} -\mathcal{J} & 0 & 0 \\ 0 & -\mathcal{J} & 0 \\ 0 & 0 & \mathcal{K} \end{pmatrix}. \quad (29)$$

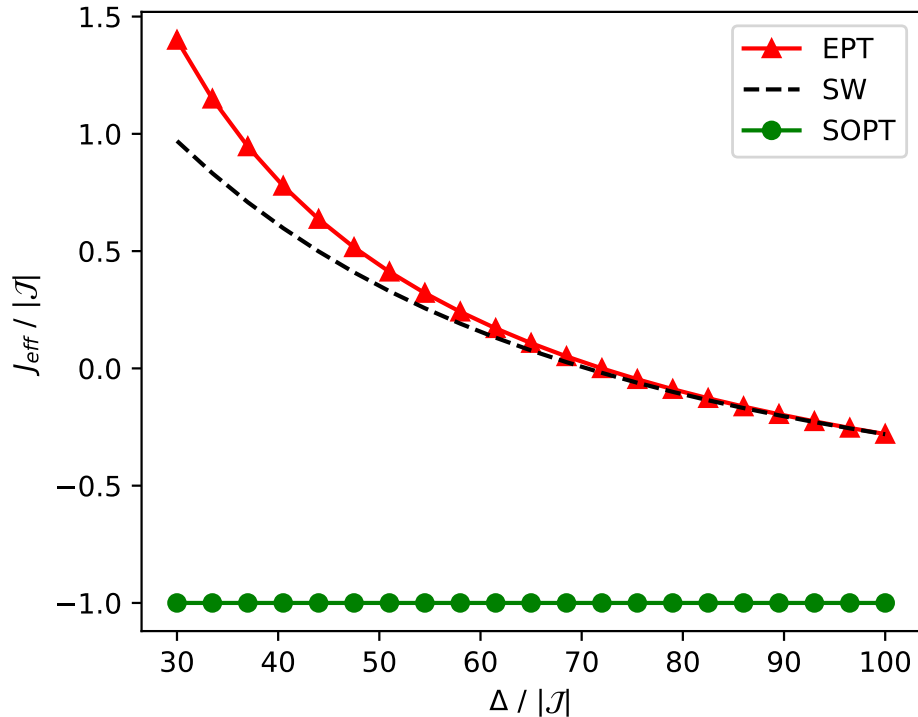


FIG. 3. Comparison of the $J = 1/2$ spin models extracted from a split $J = 3/2$ model with various splittings. The plot shows the Δ dependence of the identical diagonal components of the matrix J_{ab} in the Hamiltonian $H_{\text{eff}} = \sum_{\langle i,j \rangle} J_{ab} s_i^a s_j^b$. All off diagonal components vanish. The $J = 3/2$ model was chosen such that $J_{ab} = \text{diag}(-1, -1, -1)$ under projection, with additional coupling $K^{(i)} = \text{diag}(0, 6, 6, 6)$. All other couplings are taken to be 0. Notice that EPT at $\Delta = 36|\mathcal{J}|$ gives an antiferromagnetic Heisenberg interaction with equal magnitude to the ferromagnetic Heisenberg interaction found via projection.

Thus, the true physical theory is

$$J = \begin{pmatrix} 0 & 0 & 0 \\ 0 & 0 & 0 \\ 0 & 0 & \mathcal{J} + \mathcal{K} \end{pmatrix}. \quad (30)$$

The inter-doublet couplings generate Kitaev interactions.

The various approaches to extracting the effective $J = 1/2$ spin model from this $J = 3/2$ model are contrasted in Figure 4, in a similar manner to Figure 3. The parameters are chosen such that the EPT methods results in Equation 30 at $\Delta = 36|\mathcal{J}|$ with $\mathcal{J} < 0$ and $\mathcal{K} = 2|\mathcal{J}|$. Here again we see the agreement between the EPT and SW approaches implying that the second order perturbation theory is sufficient to reliably integrate out the exciton.

C. Heisenberg to $K\Gamma$

Extended perturbation theory can also lead to the development of off diagonal terms in the resulting spin theory. To demonstrate this consider another naive Heisenberg model which will turn into a $K\Gamma$ model with the inclusion of some inter-doublet couplings.

To produce a the Γ interaction, we take the following couplings

$$M^{(rr)} = \begin{pmatrix} 0 & 0 & 0 & 0 \\ 0 & 0 & 0 & 0 \\ 0 & 0 & 0 & 2\sqrt{|\Gamma|\Delta} \\ 0 & 0 & 2\sqrt{|\Gamma|\Delta} & 0 \end{pmatrix} \quad (31)$$

and

$$M^{(ii)} = \begin{pmatrix} 0 & 0 & 0 & 0 \\ 0 & 0 & 0 & -2\text{sign}(\Gamma)\sqrt{|\Gamma|\Delta} \\ 0 & 0 & 0 & 0 \\ 0 & -2\text{sign}(\Gamma)\sqrt{|\Gamma|\Delta} & 0 & 0 \end{pmatrix}. \quad (32)$$

With these couplings, we generate the following correction to the effective spin model

$$\delta J = \begin{pmatrix} -|\Gamma| & \Gamma & 0 \\ \Gamma & -|\Gamma| & 0 \\ 0 & 0 & 0 \end{pmatrix}. \quad (33)$$

This generates the Γ interaction. One can then use the $K^{(i)}$ to make the appropriate changes to the diagonal elements as in the previous subsection. Explicitly, the

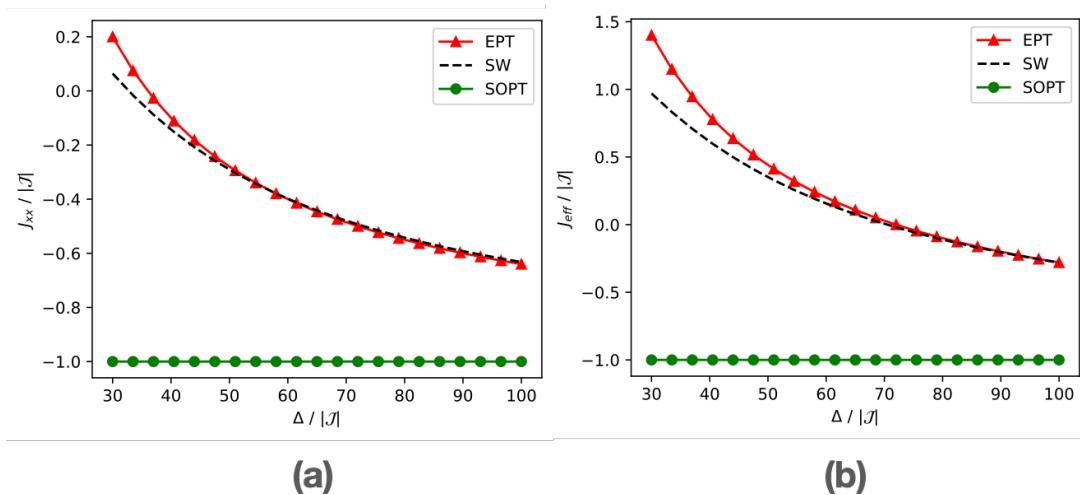


FIG. 4. Comparison of the $J = 1/2$ spin models extracted from a split $J = 3/2$ model with various splittings. The subplots show the different elements of the matrix J_{ab} in the Hamiltonian $H_{\text{eff}} = \sum_{\langle i,j \rangle} J_{ab} s_i^a s_j^b$. (a) Δ dependence of the xx -component, which is identical to the yy -component. (b) Δ dependence of the zz -component. All other components vanish. The $J = 3/2$ model was chosen such that $J_{ab} = \text{diag}(-1, -1, -1)$ under projection, with additional coupling $K^{(i)} = \text{diag}(0, 6, 6, 3)$. All other couplings are taken to be 0. Notice that EPT gives a pure Kitaev interaction at $\Delta = 36|\mathcal{J}|$.

following coupling matrix does the trick

$$K^{(i)} = \begin{pmatrix} 0 & 0 & 0 & 0 \\ 0 & \sqrt{\frac{\mathcal{K}\Delta}{2}} & 0 & 0 \\ 0 & 0 & \sqrt{\frac{\mathcal{K}\Delta}{2}} & 0 \\ 0 & 0 & 0 & -(\mathcal{J} - |\Gamma|) \sqrt{\frac{\Delta}{2\mathcal{K}}} \end{pmatrix}. \quad (34)$$

With these couplings, the physical spin model as given by the extended perturbation theory, is

$$J = \begin{pmatrix} 0 & \Gamma & 0 \\ \Gamma & 0 & 0 \\ 0 & 0 & \mathcal{J} + \mathcal{K} \end{pmatrix}. \quad (35)$$

In the spirit of Figures 3 and 4, we plot the results of various methods of integrating out the exciton in Figure 5. The parameters were chosen such that EPT results in Equation 35 at $\Delta = 36|\mathcal{J}|$ with $\mathcal{J} < 0$, $\mathcal{K} = 2|\mathcal{J}|$, and $\Gamma = |\mathcal{J}|$. The similarity between the EPT and SW lines demonstrate once again that second order perturbation theory is sufficient to integrate out the excitons for the range of Δ we consider. However, in this case, as shown in Figure 6, the J_{xz} and J_{yz} components in the SW calculation do not vanish. While these effects are small compared to the other components, it indicates that at low Δ there is some other effect, likely involving mixing between the M and K terms. Since this mixing cannot occur at second order, this suggests that higher order terms will be necessary to consider at lower values of Δ . We are only concerned with intermediate values of Δ where $J \ll \Delta$ still holds, so we are satisfied with the performance of second order perturbation theory and leave the study of higher order effects for future work.

IV. CONCLUSION

The extended perturbation theory described here is a simple and accurate technique for improving effective spin-1/2 models derived from second order perturbation theory in electron hoppings. By including the first excited multiplet on each site then integrating it out via a second perturbation step, the leading fourth order effects are included in the resulting Hamiltonian.

The effectiveness of this approach was demonstrated clearly in Section ?? for the case of d^1 and d^2 systems where it accurately followed the results of non-perturbative Schreiffer-Wolff transformations.

In addition, the results of our toy models in Section III demonstrate that this method can produce a wide variety of effects that are not included in the ordinary second order approach.

In principle, one could take either perturbation step to higher order. If we call the approach presented here as a $2 + 2$ extended perturbation theory (owing to the fact that we take the second order results of each step), we could also consider a general $n + m$ extended perturbation theory. The examples above indicate that this is not necessary for either the realistic systems or the toy models we considered. In general, we suspect that $2 + 2$ is sufficient for most systems. More involved discussions of higher orders are left for future studies.

Based on the fact that this approach is simple to implement, is accurate in describing the physics, and can produce drastic results, it should be considered for future effective Hamiltonian searches in a wider setting, especially when the ordinary second order perturbation theory does not accurately describe the observed physics.

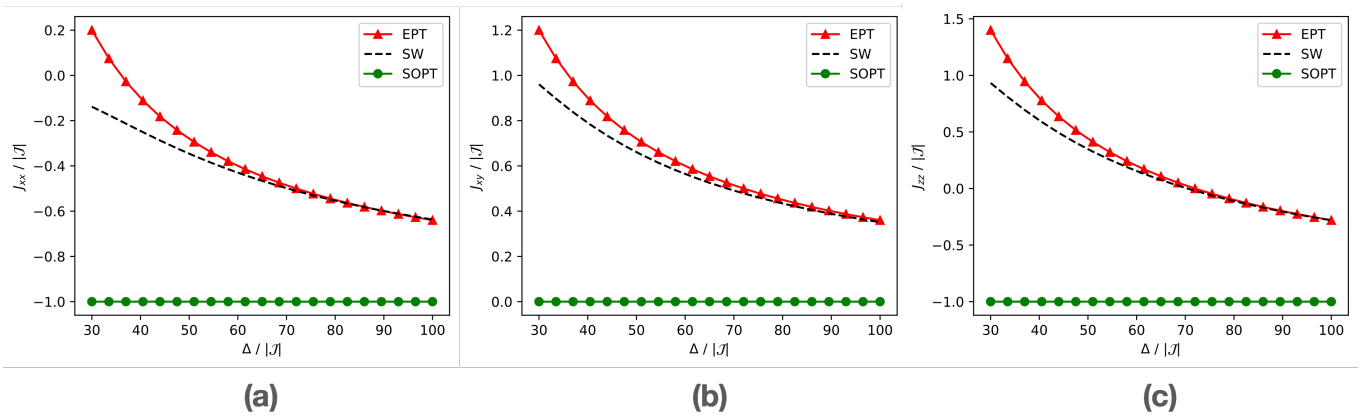


FIG. 5. Comparison of the $J = 1/2$ spin models extracted from a split $J = 3/2$ model with various splittings. The subplots represent different elements of the matrix J_{ab} in the Hamiltonian $H_{\text{eff}} = \sum_{(i,j)} J_{ab} s_i^a s_j^b$. (a) Δ dependence of the xx -element, which is identical to the yy element. (b) Δ dependence of the zz -element. (c) Δ dependence of the xy -element, which is identical to the yx -element. The remain elements have significantly smaller changes and may be seen in Figure 6. The $J = 3/2$ model was chosen such that $J_{ab} = \text{diag}(-1, -1, -1)$ under projection, with additional coupling $K^{(i)} = \text{diag}(0, 6, 6, 6)$, $M_{23}^{(rr)} = M_{32}^{(rr)} = 12$, and $M_{13}^{(ii)} = M_{31}^{(ii)} = -12$. All other couplings are taken to be 0. Notice that EPT gives a pure $K\Gamma$ interaction at $\Delta = 36|J|$.

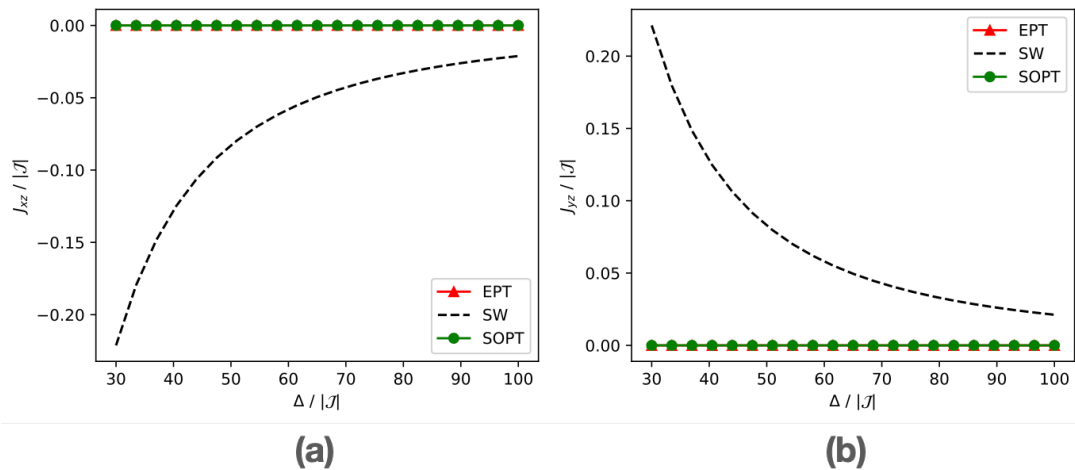


FIG. 6. (a) Comparison of the xz -component of the model in Figure 5, which is identical to the zx -component. (b) Comparison of the yz -component of the model in Figure 5, which is identical to the zy -component.

V. ACKNOWLEDGEMENTS

The authors wish to acknowledge the helpful contributions of Arijit Haldar in the early stages of this research.

This work was supported by the Natural Sciences and Engineering Research Council of Canada.

-
- [1] P. W. Anderson, The resonating valence bond state in La_2CuO_4 and superconductivity, *Science* **235**, 1196 (1987), <https://www.science.org/doi/pdf/10.1126/science.235.4793.1196>.
- [2] G. Shirane, Y. Endoh, R. J. Birgeneau, M. A. Kastner, Y. Hidaka, M. Oda, M. Suzuki, and T. Murakami, Two-dimensional antiferromagnetic quantum spin-fluid state in La_2CuO_4 , *Phys. Rev. Lett.* **59**, 1613 (1987).
- [3] S. Chakravarty, B. I. Halperin, and D. R. Nelson, Two-dimensional quantum heisenberg antiferromagnet at low temperatures, *Phys. Rev. B* **39**, 2344 (1989).
- [4] S. M. Hayden, G. Aeppli, R. Osborn, A. D. Taylor, T. G. Perring, S.-W. Cheong, and Z. Fisk, High-energy spin waves in La_2CuO_4 , *Phys. Rev. Lett.* **67**, 3622 (1991).
- [5] R. Coldea, S. M. Hayden, G. Aeppli, T. G. Perring, C. D. Frost, T. E. Mason, S.-W. Cheong, and Z. Fisk, Spin waves and electronic interactions in La_2CuO_4 , *Phys. Rev.*

- Lett. **86**, 5377 (2001).
- [6] B. J. Kim, H. Jin, S. J. Moon, J.-Y. Kim, B.-G. Park, C. S. Leem, J. Yu, T. W. Noh, C. Kim, S.-J. Oh, J.-H. Park, V. Durairaj, G. Cao, and E. Rotenberg, Novel $J_{\text{eff}} = 1/2$ mott state induced by relativistic spin-orbit coupling in sr_2iro_4 , Phys. Rev. Lett. **101**, 076402 (2008).
- [7] G. Jackeli and G. Khaliullin, Mott insulators in the strong spin-orbit coupling limit: From heisenberg to a quantum compass and kitaev models, Phys. Rev. Lett. **102**, 017205 (2009).
- [8] F. Wang and T. Senthil, Twisted hubbard model for sr_2iro_4 : Magnetism and possible high temperature superconductivity, Phys. Rev. Lett. **106**, 136402 (2011).
- [9] J. Kim, D. Casa, M. H. Upton, T. Gog, Y.-J. Kim, J. F. Mitchell, M. van Veenendaal, M. Daghofer, J. van den Brink, G. Khaliullin, and B. J. Kim, Magnetic excitation spectra of sr_2iro_4 probed by resonant inelastic x-ray scattering: Establishing links to cuprate superconductors, Phys. Rev. Lett. **108**, 177003 (2012).
- [10] B. H. Kim, G. Khaliullin, and B. I. Min, Magnetic couplings, optical spectra, and spin-orbit exciton in $5d$ electron mott insulator sr_2iro_4 , Phys. Rev. Lett. **109**, 167205 (2012).
- [11] S. Fujiyama, H. Ohsumi, T. Komesu, J. Matsuno, B. J. Kim, M. Takata, T. Arima, and H. Takagi, Two-dimensional heisenberg behavior of $J_{\text{eff}}=1/2$ isospins in the paramagnetic state of the spin-orbital mott insulator sr_2iro_4 , Phys. Rev. Lett. **108**, 247212 (2012).
- [12] I. Kimchi and A. Vishwanath, Kitaev-heisenberg models for iridates on the triangular, hyperkagome, kagome, fcc, and pyrochlore lattices, Phys. Rev. B **89**, 014414 (2014).
- [13] S. Trebst and C. Hickey, Kitaev materials, Physics Reports **950**, 1 (2022), kitaev materials.
- [14] H. Takagi, T. Takayama, G. Jackeli, G. Khaliullin, and S. E. Nagler, Concept and realization of kitaev quantum spin liquids, Nature Reviews Physics **1**, 264 (2019).
- [15] K. W. Plumb, J. P. Clancy, L. J. Sandilands, V. V. Shankar, Y. F. Hu, K. S. Burch, H.-Y. Kee, and Y.-J. Kim, $\alpha - \text{ruCl}_3$: A spin-orbit assisted mott insulator on a honeycomb lattice, Phys. Rev. B **90**, 041112 (2014).
- [16] A. Banerjee, J. Yan, J. Knolle, C. A. Bridges, M. B. Stone, M. D. Lumsden, D. G. Mandrus, D. A. Tennant, R. Moessner, and S. E. Nagler, Neutron scattering in the proximate quantum spin liquid $\alpha\text{-RuCl}_3$, Science **356**, 1055 (2017).
- [17] B. Yuan, I. Khait, G.-J. Shu, F. C. Chou, M. B. Stone, J. P. Clancy, A. Paramekanti, and Y.-J. Kim, Dirac magnons in a honeycomb lattice quantum xy magnet cotio_3 , Phys. Rev. X **10**, 011062 (2020).
- [18] M. Elliot, P. A. McClarty, D. Prabhakaran, R. D. Johnson, H. C. Walker, P. Manuel, and R. Coldea, Order-by-disorder from bond-dependent exchange and intensity signature of nodal quasiparticles in a honeycomb cobaltate, Nature Communications **12**, 3936 (2021).
- [19] S. Das, S. Voleti, T. Saha-Dasgupta, and A. Paramekanti, xy magnetism, kitaev exchange, and long-range frustration in the $J_{\text{eff}} = \frac{1}{2}$ honeycomb cobaltates, Phys. Rev. B **104**, 134425 (2021).
- [20] L. P. Regnault, C. Boullier, and J. E. Lorenzo, Polarized-neutron investigation of magnetic ordering and spin dynamics in $\text{baco}_2(\text{aso}_4)_2$ frustrated honeycomb-lattice magnet, *Heliyon*, Heliyon **4**, 10.1016/j.heliyon.2018.e00507 (2018).
- [21] H. S. Nair, J. M. Brown, E. Coldren, G. Hester, M. P. Gelfand, A. Podlesnyak, Q. Huang, and K. A. Ross, Short-range order in the quantum xxz honeycomb lattice material $\text{baco}_2(\text{PO}_4)_2$, Phys. Rev. B **97**, 134409 (2018).
- [22] J.-Q. Yan, S. Okamoto, Y. Wu, Q. Zheng, H. D. Zhou, H. B. Cao, and M. A. McGuire, Magnetic order in single crystals of $\text{na}_3\text{co}_2\text{sbo}_6$ with a honeycomb arrangement of $3d^7 \text{co}^{2+}$ ions, Phys. Rev. Materials **3**, 074405 (2019).
- [23] M. Songvilay, J. Robert, S. Petit, J. A. Rodriguez-Rivera, W. D. Ratcliff, F. Damay, V. Balédent, M. Jiménez-Ruiz, P. Lejay, E. Pachoud, A. Hadj-Azzem, V. Simonet, and C. Stock, Kitaev interactions in the co honeycomb antiferromagnets $\text{na}_3\text{co}_2\text{sbo}_6$ and $\text{na}_3\text{co}_2\text{teo}_6$, Phys. Rev. B **102**, 224429 (2020).
- [24] E. Lefrancois, M. Songvilay, J. Robert, G. Nataf, E. Jordan, L. Chaix, C. V. Colin, P. Lejay, A. Hadj-Azzem, R. Ballou, and V. Simonet, Magnetic properties of the honeycomb oxide $\text{na}_3\text{co}_2\text{teo}_6$, Phys. Rev. B **94**, 214416 (2016).
- [25] T. Halloran, F. Desrochers, E. Z. Zhang, T. Chen, L. E. Chern, Z. Xu, B. Winn, M. Graves-Brook, M. B. Stone, A. I. Kolesnikov, Y. Qiu, R. Zhong, R. Cava, Y. B. Kim, and C. Broholm, Geometrical frustration versus kitaev interactions in $\text{baco}_2\text{sub}_i2\text{i}/\text{sub}_i(\text{aso}_4\text{sub}_i4\text{i}/\text{sub}_i)\text{sub}_i2\text{i}/\text{sub}_i$, Proceedings of the National Academy of Sciences **120**, e2215509119 (2023), <https://www.pnas.org/doi/pdf/10.1073/pnas.2215509119>.
- [26] X. Zhang, Y. Xu, T. Halloran, R. Zhong, C. Broholm, R. J. Cava, N. Drichko, and N. P. Armitage, A magnetic continuum in the cobalt-based honeycomb magnet $\text{baco}_2(\text{aso}_4)_2$, Nature Materials **22**, 58 (2023).
- [27] D. Hirai and Z. Hiroi, Successive symmetry breaking in a $j_{\text{eff}} = 3/2$ quartet in the spin-orbit coupled insulator $\text{ba}_2\text{mgreo}_6$, Journal of the Physical Society of Japan **88**, 064712 (2019).
- [28] D. Hirai, H. Sagayama, S. Gao, H. Ohsumi, G. Chen, T.-h. Arima, and Z. Hiroi, Detection of multipolar orders in the spin-orbit-coupled $5d$ mott insulator $\text{ba}_2\text{mgreo}_6$, Phys. Research **2**, 022063 (2020).
- [29] D. D. Maharaj, G. Sala, M. B. Stone, E. Kermarrec, C. Ritter, F. Fauth, C. A. Marjerrison, J. E. Greedan, A. Paramekanti, and B. D. Gaulin, Octupolar versus néel order in cubic $5d^2$ double perovskites, Phys. Rev. Lett. **124**, 087206 (2020).
- [30] D. D. Maharaj, G. Sala, M. B. Stone, E. Kermarrec, C. Ritter, F. Fauth, C. A. Marjerrison, J. E. Greedan, A. Paramekanti, and B. D. Gaulin, Octupolar versus néel order in cubic $5d^2$ double perovskites, Phys. Rev. Lett. **124**, 087206 (2020).
- [31] A. Paramekanti, D. D. Maharaj, and B. D. Gaulin, Octupolar order in d -orbital mott insulators, Phys. Rev. B **101**, 054439 (2020).
- [32] S. Voleti, D. D. Maharaj, B. D. Gaulin, G. Luke, and A. Paramekanti, Multipolar magnetism in d -orbital systems: Crystal field levels, octupolar order, and orbital loop currents, Phys. Rev. B **101**, 155118 (2020).
- [33] S. Voleti, A. Haldar, and A. Paramekanti, Octupolar order and ising quantum criticality tuned by strain and dimensionality: Application to d -orbital mott insulators, Phys. Rev. B **104**, 174431 (2021).
- [34] We take the convention that σ^0 is the 2×2 identity matrix and $\sigma^1 = \sigma^x$, $\sigma^2 = \sigma^y$, and $\sigma^3 = \sigma^z$.

- [35] A. Georges, L. d. Medici, and J. Mravlje, Strong correlations from Hund's coupling, Annual Review of Condensed Matter Physics **4**, 137 (2013).
- [36] G. Jackeli and G. Khaliullin, Mott insulators in the strong spin-orbit coupling limit: From Heisenberg to a quantum compass and Kitaev models, Phys. Rev. Lett. **102**, 017205 (2009).
- [37] The exact form of these elements depends on the choice of index i when defining $M^{(rr)}$ and $M^{(ii)}$. The values of these elements will have little bearing on the procedure for finding $K^{(i)}$, so we do not give it explicitly.

Appendix A: Extended Perturbation Theory Details

In this appendix, we fill in the details in the derivation of Eqns. (7) and (8). As mentioned in the main text, we assume that we have an interaction matrix 16×16 matrix $\mathcal{H}_{3/2}$ that contains all second order in H_T contributions to the interactions between pseudospins and excitons on the two sites. We split up the terms of $\mathcal{H}_{3/2}$ as follows:

$$\begin{aligned} \mathcal{H}_{3/2} &= H_0 + \mathcal{V}_J \\ &= H_0 + \mathcal{V}_J^{(\eta\eta)} + \mathcal{V}_J^{(\eta\xi)} + \mathcal{V}_J^{(\xi\xi)} \\ &\quad + \mathcal{V}_J^{(\eta\tau)} + \mathcal{V}_J^{(\tau\tau)} + \mathcal{V}_J^{(\tau\xi)} \end{aligned} \quad (\text{A1})$$

Here H_0 is the matrix that splits the spectrum on each site, namely

$$H_0 = \Delta (\tau^0 \otimes \eta^0 + \eta^0 \otimes \tau^0 + 2 \tau^0 \otimes \tau^0). \quad (\text{A2})$$

Each $\mathcal{V}_J^{(st)}$ denotes the collection of terms that couple s and t operators on each site. For completeness, we write each one out fully, but as stated in the main text only $\mathcal{V}_J^{(\eta\eta)}$, $\mathcal{V}_J^{(\eta\xi)}$, and $\mathcal{V}_J^{(\xi\xi)}$ can contribute to the effective $J = 1/2$ Hamiltonian at second order. By our conventions,

$$\mathcal{V}_J^{(\eta\eta)} = J_{ab}^{(\eta\eta)} \eta^a \otimes \eta^b, \quad (\text{A3})$$

$$\begin{aligned} \mathcal{V}_J^{(\eta\xi)} &= K_{ab}^{(r)} (\eta^a \otimes \xi_r^b + \xi_r^b \otimes \eta^a) \\ &\quad + K_{ab}^{(i)} (\eta^a \otimes \xi_i^b + \xi_i^b \otimes \eta^a), \end{aligned} \quad (\text{A4})$$

$$\begin{aligned} \mathcal{V}_J^{(\xi\xi)} &= M_{ab}^{(rr)} \xi_r^a \otimes \xi_r^b + M_{ab}^{(ii)} \xi_i^a \otimes \xi_i^b \\ &\quad + M_{ab}^{(ri)} (\xi_r^a \otimes \xi_i^b + \xi_i^b \otimes \xi_r^a), \end{aligned} \quad (\text{A5})$$

$$\mathcal{V}_J^{(\eta\tau)} = J_{ab}^{(\eta\tau)} (\eta^a \otimes \tau^b + \tau^b \otimes \eta^a), \quad (\text{A6})$$

$$\mathcal{V}_J^{(\tau\tau)} = J_{ab}^{(\tau\tau)} \tau^a \otimes \tau^b, \quad (\text{A7})$$

and

$$\begin{aligned} \mathcal{V}_J^{(\tau\xi)} &= N_{ab}^{(r)} (\tau^a \otimes \xi_r^b + \xi_r^b \otimes \tau^a) \\ &\quad + N_{ab}^{(i)} (\tau^a \otimes \xi_i^b + \xi_i^b \otimes \tau^a). \end{aligned} \quad (\text{A8})$$

Here the J , K , M , and N symbols represent 4×4 matrices of real-valued coefficients that determine the interaction strengths of all the possible interactions. The indices a and b are meant to be summed over $\{0, 1, 2, 3\}$ according to Einstein summation notation, whereas r and i are merely labels for the ξ_r and ξ_i operators and should not be summed over. We assume inversion symmetry between the sites, making $J^{\eta\eta}$, $J^{\tau\tau}$, $M^{(rr)}$, and $M^{(ii)}$ symmetric matrices. We will assume for the sake of perturbation theory that $J, K, M, N \ll \Delta$.

With just H_0 , the $|J_z| = 1/2$ subspace is entirely trivial; no interactions occur between sites and on each site the two states are perfectly degenerate. Therefore, our use of degenerate perturbation theory is justified. Let $P_0 = \eta^0 \otimes \eta^0$ denote the projector onto the subspace with $|J_z| = 1/2$ on both sites, and $P_1 = I - P_0$. At first order, we get

$$\begin{aligned} H_{\text{eff}}^{[1]} &= P_0 \mathcal{V}_J P_0 \\ &= \mathcal{V}_J^{(\eta\eta)}. \end{aligned} \quad (\text{A9})$$

At this order, only $\mathcal{V}_J^{(\eta\eta)}$ can contribute. This reproduces the standard interaction Hamiltonian obtained through merely projecting to the lower doublet.

To get our extended perturbation theory result, we look at the second order correction given by Eqn. (1),

$$H_{\text{eff}}^{[2]} = -P_0 \mathcal{V}_J P_1 \frac{1}{H_0} P_1 \mathcal{V}_J P_0 \quad (\text{A10})$$

With a little algebra one can show that this splits into two terms $H_{\text{eff}}^{[2]} = H_K^{[2]} + H_M^{[2]}$ with

$$H_K^{[2]} = -P_0 \mathcal{V}^{(\eta\xi)} P_1 \frac{1}{H_0} P_1 \mathcal{V}^{(\eta\xi)} P_0 \quad (\text{A11})$$

and

$$H_M^{[2]} = -P_0 \mathcal{V}^{(\xi\xi)} P_1 \frac{1}{H_0} P_1 \mathcal{V}^{(\xi\xi)} P_0. \quad (\text{A12})$$

Notice that $P_0 \mathcal{V}^{(\eta\xi)} P_1 = P_0 \mathcal{V}^{(\eta\xi)}$ vanishes on all states except for those that have $|J_z| = 1/2$ on one site and $|J_z| = 3/2$ on the other. Hence, the only non-vanishing contribution sees $1/H_0$ as $1/\Delta$. Using this we can simplify our equation greatly,

$$H_K^{[2]} = -\frac{1}{\Delta} P_0 \left(\mathcal{V}^{(\eta\xi)} \right)^2 P_0. \quad (\text{A13})$$

Similarly, $P_0 \mathcal{V}^{(\xi\xi)} P_1 = P_0 \mathcal{V}^{(\xi\xi)}$ kills all states except for those with $|J_z| = 3/2$ on both sites, allowing the simplification

$$H_M^{[2]} = -\frac{1}{2\Delta} P_0 \left(\mathcal{V}^{(\xi\xi)} \right)^2 P_0. \quad (\text{A14})$$

By writing the ξ operators explicitly as tensor products of Pauli matrices and recalling that we defined lambda through $\sigma^a \sigma^b = \lambda^{abc} \sigma^c$, we can rewrite $H_K^{[2]} =$

$(\delta J_K)_{ab} \sigma^a \otimes \sigma^b$ and $H_M^{[2]} = (\delta J_M)_{ab} \sigma^a \otimes \sigma^b$. Following this procedure gives

$$(\delta J_K)_{ab} = -\frac{1}{2\Delta} \left(K_{cd}^{(r)} - iK_{cd}^{(i)} \right) \left(K_{ef}^{(r)} + iK_{ef}^{(i)} \right) \times (\lambda_{cea}\lambda_{dfb} + \lambda_{ceb}\lambda_{dfa}) \quad (\text{A15})$$

and

$$(\delta J_M)_{ab} = -\frac{1}{8\Delta} \left(M_{cd}^{(rr)} - M_{cd}^{(ii)} - iM_{cd}^{(ri)} - iM_{cd}^{(ri)} \right) \times \left(M_{ef}^{(rr)} - M_{ef}^{(ii)} + iM_{ef}^{(ri)} + iM_{ef}^{(ri)} \right) \lambda_{cea}\lambda_{dfb} \quad (\text{A16})$$

as presented in the main text. Therefore, we can describe our effective Hamiltonian as

$$H_{\text{eff}} = (J_{\text{eff}})_{ab} \sigma^a \otimes \sigma^b = \left(J^{(\eta\eta)} + \delta J_K + \delta J_M \right)_{ab} \sigma^a \otimes \sigma^b. \quad (\text{A17})$$

Appendix B: Proof of surjectivity of the extended perturbation theory equations

In this section, we prove the claim made in Section III that the extended perturbation theory can create any change in the spin model. In other words, Equations (7) and (8), which determine δJ , are surjective onto the set of symmetric 3×3 matrices. We will prove this claim by starting with an arbitrary δJ and constructing $K^{(i)}$, $M^{(rr)}$, and $M^{(ii)}$ couplings that produce δJ . An important feature of this construction is that it will only involve non-zero coefficients for couplings which preserve the time-reversal and exchange symmetries. Hence, there are no symmetry restrictions to finding these couplings in nature.

Consider an arbitrary symmetric 3×3 matrix, δJ . For concreteness, we label the elements of this matrix as

$$\delta J = \begin{pmatrix} k1 & m3 & m2 \\ m3 & k2 & m1 \\ m2 & m1 & k3 \end{pmatrix}. \quad (\text{B1})$$

Here we have been intentionally suggestive with our labels. Indeed the off-diagonal m_i elements will be set by our choice of $M^{(rr)}$ and $M^{(ii)}$, then the diagonal will be set by our choice of $K^{(i)}$.

Starting with the off-diagonal elements, the simplest case is that $m_1 = m_2 = m_3 = 0$. In this case, we can set $M^{(rr)} = M^{(ii)} = 0$ and move on to dealing with the diagonal elements. Otherwise, suppose $m_i \neq 0$ for some $i \in \{1, 2, 3\}$. It will be useful to define the following

matrix-valued functions

$$\begin{aligned} M_1(a, b) &= \begin{pmatrix} 0 & 0 & 0 & 0 \\ 0 & b & 0 & 0 \\ 0 & 0 & 0 & -a \\ 0 & 0 & -a & 0 \end{pmatrix} \\ M_2(a, b) &= \begin{pmatrix} 0 & 0 & 0 & 0 \\ 0 & 0 & 0 & -a \\ 0 & 0 & b & 0 \\ 0 & -a & 0 & 0 \end{pmatrix} \\ M_3(a, b) &= \begin{pmatrix} 0 & 0 & 0 & 0 \\ 0 & 0 & -a & 0 \\ 0 & -a & 0 & 0 \\ 0 & 0 & 0 & b \end{pmatrix}, \end{aligned} \quad (\text{B2})$$

where a and b are real numbers. In what follows, all arithmetic involving indices is modulo 3.

Consider setting $M^{(rr)} = M_{i+1}(a, b)$, $M^{(ii)} = M_{i+2}(c, d)$, $M^{(ri)} = 0$, and $M^{(ir)} = 0$, for some real numbers a, b, c , and d . Plugging these into Equation A16 and equating the off-diagonal elements to the off-diagonal components of δJ , one finds the following system of equations

$$\begin{aligned} m_i &= -\frac{ac}{4\Delta} \\ m_{i+1} &= \frac{ab}{4\Delta} \\ m_{i+2} &= \frac{cd}{4\Delta}. \end{aligned} \quad (\text{B3})$$

A solution to this system of equations is given by

$$\begin{aligned} a &= -2\text{sign}(m_i)\sqrt{|m_i|\Delta} \\ b &= -2\text{sign}(m_i)m_{i+1}\sqrt{\frac{\Delta}{|m_i|}} \\ c &= 2\sqrt{|m_i|\Delta} \\ d &= 2m_{i+2}\sqrt{\frac{\Delta}{|m_i|}}. \end{aligned} \quad (\text{B4})$$

Hence, to have δJ_M have the desired off-diagonal elements, define

$$\begin{aligned} M^{(rr)} &= \\ M_{i+1} &\left(-2\text{sign}(m_i)\sqrt{|m_i|\Delta}, -2\text{sign}(m_i)m_{i+1}\sqrt{\frac{\Delta}{|m_i|}} \right) \end{aligned} \quad (\text{B5})$$

and

$$M^{(ii)} = M_{i+2} \left(2\sqrt{|m_i|\Delta}, 2m_{i+2}\sqrt{\frac{\Delta}{|m_i|}} \right). \quad (\text{B6})$$

In general, the resulting δJ_M will have non-zero diagonal elements[37], so to fully reproduce the desired δJ ,

we need to find $K^{(r)}$ and $K^{(i)}$ such that

$$\delta J_K = \begin{pmatrix} k_1 - \delta J_{M,11} & 0 & 0 \\ 0 & k_2 - \delta J_{M,22} & 0 \\ 0 & 0 & k_3 - \delta J_{M,33} \end{pmatrix}. \quad (\text{B7})$$

For simplicity of notation, we define $\tilde{k}_i = k_i - \delta J_{M,ii}$. Consider setting $K^{(r)} = 0$ and

$$K^{(i)} = \begin{pmatrix} a_0 & 0 & 0 & 0 \\ 0 & a_1 & 0 & 0 \\ 0 & 0 & a_2 & 0 \\ 0 & 0 & 0 & a_3 \end{pmatrix}, \quad (\text{B8})$$

with $a_0, a_1, a_2, a_3 \in \mathbb{R}$. Evaluating δJ_K and equating with the desired form gives the following system of equations

$$\begin{aligned} a_0 a_1 - a_2 a_3 &= -\frac{2}{\Delta} \tilde{k}_1 \equiv \kappa_1 \\ a_0 a_2 - a_3 a_1 &= -\frac{2}{\Delta} \tilde{k}_2 \equiv \kappa_2 \\ a_0 a_3 - a_1 a_2 &= -\frac{2}{\Delta} \tilde{k}_3 \equiv \kappa_3. \end{aligned} \quad (\text{B9})$$

A useful trick for finding a general solution to these equa-

tions is to set

$$\begin{aligned} a_0 &= b - c \\ a_1 &= b + c \\ a_2 &= f + e \\ a_3 &= f - e \end{aligned} \quad (\text{B10})$$

for some real numbers $b, c, e,$ and f . This changes the Equations B9 to

$$\begin{aligned} b^2 - c^2 - e^2 + f^2 &= \kappa_1 \\ -2ce + 2bf &= \kappa_2 \\ -2ce - 2bf &= \kappa_3 \end{aligned} \quad (\text{B11})$$

The last two equations imply that

$$\begin{aligned} ce &= -\frac{1}{4}(\kappa_2 + \kappa_3) \equiv \kappa_+ \\ bf &= \frac{1}{4}(\kappa_2 - \kappa_3) \equiv \kappa_-. \end{aligned} \quad (\text{B12})$$

We are free to choose our solution such that $e, f \neq 0$, in which case we may combine Equations B12 with the first equation of B11 to find

$$f^2 + \frac{\kappa_+^2}{f^2} - e^2 - \frac{\kappa_-^2}{e^2} = \kappa_1. \quad (\text{B13})$$

This equation can be solved with

$$f = \begin{cases} \sqrt{\kappa_1 + |\kappa_+| + |\kappa_-| + \sqrt{(\kappa_1 + |\kappa_+| + |\kappa_-|)^2 - 4\kappa_-^2}} & \kappa_1 \geq 0 \\ \sqrt{\frac{|\kappa_1|}{2} + |\kappa_+| + |\kappa_-| + \sqrt{\left(\frac{|\kappa_1|}{2} + |\kappa_+| + |\kappa_-|\right)^2 - 4\kappa_-^2}} & \kappa_1 < 0 \end{cases} \quad (\text{B14})$$

and

$$e = \begin{cases} \sqrt{\frac{\kappa_1}{2} + |\kappa_+| + |\kappa_-| + \sqrt{\left(\frac{\kappa_1}{2} + |\kappa_+| + |\kappa_-|\right)^2 - 4\kappa_+^2}} & \kappa_1 \geq 0 \\ \sqrt{|\kappa_1| + |\kappa_+| + |\kappa_-| + \sqrt{(|\kappa_1| + |\kappa_+| + |\kappa_-|)^2 - 4\kappa_+^2}} & \kappa_1 < 0 \end{cases}. \quad (\text{B15})$$

These solutions can then be used to find $b = \kappa_-/f$ and $c = \kappa_+/e$, and subsequently $a_0 = b - c$, $a_1 = b + c$, $a_2 = e + f$, and $a_3 = e - f$. The resulting $K^{(i)}$ gives the desired δJ_K , completing the proof.

Appendix C: Relations between operators

Here we provide useful details about the operators used in the main text to describe $J = 3/2$ degrees of freedom. The definition of the multipole basis in terms of the dipole operators, which form a $J = 3/2$ representation of the $\mathfrak{su}(2)$ algebra, is presented in Table I. These definitions are well-known; we include them for the sake of completeness and transparency with our conventions. The relationship between this basis and the basis defined in Equations (2) and (3) is given in Table II.

Moment	Symmetry	Symbol	Expression
Dipole	T_1	J_x	
		J_y	
		J_z	
Quadrupole	T_2	Q_{yz}	$\frac{1}{\sqrt{3}} \overline{J_y J_z}$
		Q_{zx}	$\frac{1}{\sqrt{3}} \overline{J_z J_x}$
		Q_{xy}	$\frac{1}{\sqrt{3}} \overline{J_x J_y}$
	E	$Q_{x^2-y^2}$	$\frac{1}{\sqrt{3}} (J_x^2 - J_y^2)$
		Q_{z^2}	$\frac{1}{3} (3J_z^2 - \mathbf{J}^2)$
Octupole	A_2	T_{xyz}	$\frac{2}{3\sqrt{3}} \overline{J_x J_y J_z}$
	T_1	T_x^a	$\frac{2}{3} (J_x)^3 - \frac{1}{3} (\overline{J_x (J_y)^2} + \overline{(J_z)^2 J_x})$
		T_y^a	$\frac{2}{3} (J_y)^3 - \frac{1}{3} (\overline{J_y (J_z)^2} + \overline{(J_x)^2 J_y})$
		T_z^a	$\frac{2}{3} (J_z)^3 - \frac{1}{3} (\overline{J_z (J_x)^2} + \overline{(J_y)^2 J_z})$
	T_2	T_x^b	$\frac{2}{3\sqrt{3}} (\overline{J_x (J_y)^2} - \overline{(J_z)^2 J_x})$
		T_y^b	$\frac{2}{3\sqrt{3}} (\overline{J_y (J_z)^2} - \overline{(J_x)^2 J_y})$
		T_z^b	$\frac{2}{3\sqrt{3}} (\overline{J_z (J_x)^2} - \overline{(J_y)^2 J_z})$

TABLE I. The definition of the various multipole operators for a $J = 3/2$ system in terms of the dipole operators. These operators form a useful basis of $\mathfrak{su}(4)$.

Type	Symbol	Expression
Lower Doublet	η^0	$-\frac{1}{2}Q_{z^2} + \frac{1}{2}$
	η^x	$\frac{2}{5}J_x + \frac{3}{10}T_x^a + \frac{\sqrt{3}}{4}T_x^b$
	η^y	$\frac{2}{5}J_y + \frac{3}{10}T_y^a - \frac{\sqrt{3}}{4}T_y^b$
	η^z	$\frac{1}{5}J_z + \frac{3}{5}T_z^a$
Upper Doublet	τ^0	$\frac{1}{2}Q_{z^2} + \frac{1}{2}$
	τ^x	$\frac{1}{2}T_x^a - \frac{\sqrt{3}}{4}T_x^b$
	τ^y	$-\frac{1}{2}T_y^a - \frac{\sqrt{3}}{4}T_y^b$
	τ^z	$-\frac{3}{5}J_z + \frac{1}{5}T_z^a$
Mixing Between Doublets	ξ_r^0	$\frac{\sqrt{6}}{5}J_x - \frac{\sqrt{3}}{5\sqrt{2}}T_x^a - \frac{1}{2\sqrt{2}}T_x^b$
	ξ_r^x	$\frac{1}{\sqrt{2}}Q_{x^2-y^2}$
	ξ_r^y	$\frac{1}{\sqrt{2}}Q_{xy}$
	ξ_r^z	$\frac{1}{\sqrt{2}}Q_{zx}$
	ξ_i^0	$-\frac{1}{\sqrt{2}}Q_{yz}$
	ξ_i^x	$-\frac{1}{\sqrt{2}}T_{xyz}$
	ξ_i^y	$\frac{1}{\sqrt{2}}T_z^b$
	ξ_i^z	$-\frac{\sqrt{6}}{5}J_y + \frac{\sqrt{3}}{5\sqrt{2}}T_y^a - \frac{1}{2\sqrt{2}}T_y^b$

TABLE II. The relation between the magnetic multipole operator basis for a $J = 3/2$ system and the basis introduced in Equations (2) and (3). Here we have included the identity operator with the multipole basis, so these basis describe the 16-dimensional space, $u(4)$.